

## SUPPORTING INFORMATION

### **Rare-Earth-free Magnets: Enhancing Magnetic Anisotropy and Spin Exchange Toward High- $T_C$ $\text{Hf}_2\text{M}\text{Ir}_5\text{B}_2$ ( $M = \text{Mn}, \text{Fe}$ )**

Pritam Shankhari,<sup>a</sup> Oliver Janka,<sup>b,c</sup> Rainer Pöttgen,<sup>c</sup> Boniface P. T. Fokwa\*,<sup>a, d</sup>

<sup>a</sup> Department of Chemistry, University of California, Riverside, CA 92521, United States

<sup>b</sup> Anorganische Festkörperchemie, Universität des Saarlandes, Campus C 4 1, D-66123  
Saarbrücken, Germany

<sup>c</sup> Institut für Anorganische und Analytische Chemie, Westfälische Wilhelms-Universität  
Münster, Corrensstrasse 30, D-48149 Münster, Germany

<sup>d</sup> Department of Chemical and Environmental Engineering, University of California, Riverside, CA 92521, United States

## Experimental Procedure

The starting materials used for the synthesis of the  $\text{Hf}_2\text{M}\text{Ir}_5\text{B}_2$  ( $M = \text{Fe}, \text{Mn}$ ) phases were purchased elemental powders of Hf (99.6%), Mn (99.99%), Fe (99.995%), Ir (99.9%), and B (99% amorphous and crystalline). The elements were weighed in the desired atomic ratio, mixed well (total mass around 0.3 g), and the mixture was pressed into a pellet inside a glove box. The pellet was arc-melted under an argon atmosphere using a Schlenk line. The argon gas was purified prior to use over silica gel, molecular sieves, and titanium sponge (at 950 K). The melting was performed on a water-cooled copper crucible using a tungsten tip as the second electrode, where the pellet was re-melted for a few seconds with a direct current of 20 Amperes until a homogeneous melting was achieved (prolonged melting will evaporate manganese). During the handling, sample preparation, manipulation and synthesis, tungsten carbide die sets, agate mortar-pestle were used to avoid any magnetic contaminations. The synthesized phase was stable in the air as a compact bulk as well as finely ground powders.

Powder X-ray diffraction data (PXRD) of synthesized compounds was collected at room temperature, using a Rigaku MiniFlex 600 diffractometer (Cu- $K\alpha_1$  radiation ( $\lambda = 1.5405 \text{ \AA}$ ), Ge monochromator, image plate detector, and silicon standard). Additionally, the PXRD pattern of the pulverized sample of  $\text{Hf}_2\text{MnIr}_5\text{B}_2$ , used for the magnetic measurements, was recorded at room temperature on a D8-A25-Advance diffractometer (Bruker, Karlsruhe, Germany) in Bragg-Brentano  $\theta$ - $\theta$ -geometry (goniometer radius 280 mm) with Cu  $K\alpha$ -radiation ( $\lambda = 1.540596 \text{ \AA}$ ). The sample were prepared on a zero-background holder. A 12  $\mu\text{m}$  Ni foil working as  $K\beta$  filter and a variable divergence slit were mounted at the primary beam side. A LYNXEYE detector with 192 channels was used at the secondary beam side. Experiments were carried out in a  $2\theta$  range of 10 to 120° with a step size of 0.013° and a total scan time of 4h. The recorded data was analyzed with the Bruker TOPAS 5.0 software [1].

Energy-dispersive X-ray spectroscopy (EDS) was carried out on an ultra-high-resolution low-energy system of the type Nova NanoSEM450 equipped with a 50mm<sup>2</sup> X-Max 50 SD EDX detector.

For the low temperature magnetization measurements (3-300 K), the powdered samples of the  $\text{Hf}_2\text{FeIr}_5\text{B}_2$  and  $\text{Hf}_2\text{MnIr}_5\text{B}_2$  were filled in polyethylene (PE) capsules that were attached to the sample holder rod. For the high-temperature measurements (300-950 K), the powders of the  $\text{Hf}_2\text{FeIr}_5\text{B}_2$  and  $\text{Hf}_2\text{MnIr}_5\text{B}_2$  were pressed to small pellets ( $\varnothing$  2 mm) under a pressure of 100 bar. Pieces of these pellets were subsequently obtained by careful fragmentation. One fragment was mounted on a high-temperature sample holder using Zircar® cement, followed by careful wrapping in Cu-foil. The sample was then attached to the sample holder rod of a Vibrating Sample Magnetometer (VSM) for measuring the magnetization  $M(T, H)$  in a Quantum Design Physical Property Measurement System (PPMS).

**Table S1.** Relative energies of different magnetic models compared to the most stable one (**in bold**) obtained from VASP calculations.

Compound	Relative energy compared to the most stable model (meV/f.u.)			
	FM	AFM1	AFM2	NM
Hf <sub>2</sub> FeIr <sub>5</sub> B <sub>2</sub>	<b>0.00</b>	40.19	96.17	1106.15
Hf <sub>2</sub> MnIr <sub>5</sub> B <sub>2</sub>	-60.01	<b>0.00</b>	242.47	1507.31

**Table S2.** Calculated atomic and total magnetic moments for Hf<sub>2</sub>FeIr<sub>5</sub>B<sub>2</sub> and Hf<sub>2</sub>MnIr<sub>5</sub>B<sub>2</sub> in the FM model.

Compound	Fe/Mn (2a)	Hf (4g)	Ir (2c)	Ir (8j)	B (4g)	Total
Hf <sub>2</sub> FeIr <sub>5</sub> B <sub>2</sub> (FM)	+2.93	-0.02	+0.07	+0.17	+0.01	+3.62
Hf <sub>2</sub> MnIr <sub>5</sub> B <sub>2</sub> (FM)	+3.34	+0.03	+0.03	+0.11	-0.01	+3.83

**Table S3.** Valence electrons (VE), and relative energies for different magnetic models compared to the most stable one obtained from VASP calculations for all Fe- and Mn-based compounds in Ti<sub>3</sub>Co<sub>5</sub>B<sub>2</sub> structure type. The most stable model is the ground state (with 0 meV/f.u. energy).

Compound	VE	Relative energy. The most stable model is given in boldface (meV/f.u.)			Reference
		FM	AFM1	AFM2	
<b>Fe-based compounds</b>					
Hf <sub>2</sub> FeIr <sub>5</sub> B <sub>2</sub>	67	<b>0.00</b>	40.19	96.17	This work
Ti <sub>2</sub> FeRh <sub>5</sub> B <sub>2</sub>	67	<b>0.00</b>	3.74	11.70	[24]
Ti <sub>2</sub> FeCo <sub>5</sub> B <sub>2</sub>	67	<b>0.00</b>	53.09	199.07	[24]
Hf <sub>2</sub> FeCo <sub>5</sub> B <sub>2</sub>	67	<b>0.00</b>	58.88	155.79	[24]
Hf <sub>2</sub> FeRu <sub>5</sub> B <sub>2</sub>	62	38.30	<b>0.00</b>	38.40	[33]
Zr <sub>2</sub> FeRu <sub>5</sub> B <sub>2</sub>	62	44.50	<b>0.00</b>	44.25	[33]
Ti <sub>2</sub> FeRu <sub>4</sub> RhB <sub>2</sub>	63	30.55	<b>0.00</b>	22.22	[24]
Sc <sub>2</sub> FeRu <sub>3</sub> Ir <sub>2</sub> B <sub>2</sub>	62	36.77	<b>0.00</b>	10.77	[24]
<b>Mn-based compounds</b>					
Hf <sub>2</sub> MnIr <sub>5</sub> B <sub>2</sub>	66	60.01	<b>0.00</b>	242.47	This work
TiMnCo <sub>5</sub> B <sub>2</sub>	66	9.82	<b>0.00</b>	144.69	[24]
Hf <sub>2</sub> MnCo <sub>5</sub> B <sub>2</sub>	66	<b>0.00</b>	5.46	194.77	[24]
Hf <sub>2</sub> MnRu <sub>5</sub> B <sub>2</sub>	61	<b>0.00</b>	1.92	33.05	[32]
Zr <sub>2</sub> MnRu <sub>5</sub> B <sub>2</sub>	61	2.40	<b>0.00</b>	49.95	[33]

**Table S4.** Results of the *Rietveld* refinements of the powder XRD data for Hf<sub>2</sub>FeIr<sub>5</sub>B<sub>2</sub> and Hf<sub>2</sub>MnIr<sub>5</sub>B<sub>2</sub>.

Phase	Hf <sub>2</sub> FeIr <sub>5</sub> B <sub>2</sub>	Hf <sub>2</sub> MnIr <sub>5</sub> B <sub>2</sub>
Refined composition	Hf <sub>2</sub> Fe <sub>0.64(2)</sub> Ir <sub>5.36(2)</sub> B <sub>2</sub>	Hf <sub>2</sub> Mn <sub>0.82(2)</sub> Ir <sub>5.18(2)</sub> B <sub>2</sub>
Space group; <i>Z</i>	<i>P4/mbm</i> (no. 127), 2	
Profile function	pseudo-Voigt	
$\theta$ range (degrees)	10 - 90	
Data Collection Step (degree)	0.02	
No of Data Points	4000	
<i>a</i> (Å)	9.0969(7)	9.1845(6)
<i>c</i> (Å)	3.2039(3)	3.2146(2)
<i>V</i> (Å <sup>3</sup> )	265.13(4)	271.17(3)
<i>R</i> <sub>f</sub> , <i>R</i> <sub>Bragg</sub>	7.18, 9.87	4.12, 6.43
Weight fraction (wt %)	68%	80%
Side Phase; wt %; lattice parameter	HfIr <sub>3</sub> B <sub>0.5</sub> ( <i>Pm-3m</i> , no. 221); 32% <i>a</i> = 3.9798(3) Å	HfIr <sub>3</sub> B <sub>0.5</sub> ( <i>Pm-3m</i> , no. 221); 20% <i>a</i> = 3.9848(2) Å

**Table S5.** Atomic positions and site occupation factors (SOF) for Hf<sub>2</sub>FeIr<sub>5</sub>B<sub>2</sub> and Hf<sub>2</sub>MnIr<sub>5</sub>B<sub>2</sub>. The figure below shows the location of different atom and their labels within the unit cell (viewed along the *c*-direction). The position of the light element boron was refined separately after refining then fixing the metal positions. Details crystallographic information are provided in CIFs.

Atom label	Wyckoff position	<i>x</i>	<i>y</i>	<i>z</i>	SOF
Refined composition Hf <sub>2</sub> Fe <sub>0.64(2)</sub> Ir <sub>5.36(2)</sub> B <sub>2</sub>					
Hf1	4g	0.1836(5)	0.6836(5)	0	1
Ir1	8j	0.0654(4)	0.2238(5)	0.5	1
Ir2	2c	0	0.5	0.5	1
Ir3	2a	0	0	0	0.36(2)
Fe1	2a	0	0	0	0.64(2)
B1	4g	0.632(7)	0.132(7)	0	1
Refined composition Hf <sub>2</sub> Mn <sub>0.82(2)</sub> Ir <sub>5.18(2)</sub> B <sub>2</sub>					
Hf1	4g	0.1754(4)	0.6754(4)	0	1
Ir1	8j	0.0686(3)	0.2158(3)	0.5	1
Ir2	2c	0	0.5	0.5	1
Ir3	2a	0	0	0	0.18(2)
Mn1	2a	0	0	0	0.82(2)
B1	4g	0.611(6)	0.111(8)	0	1

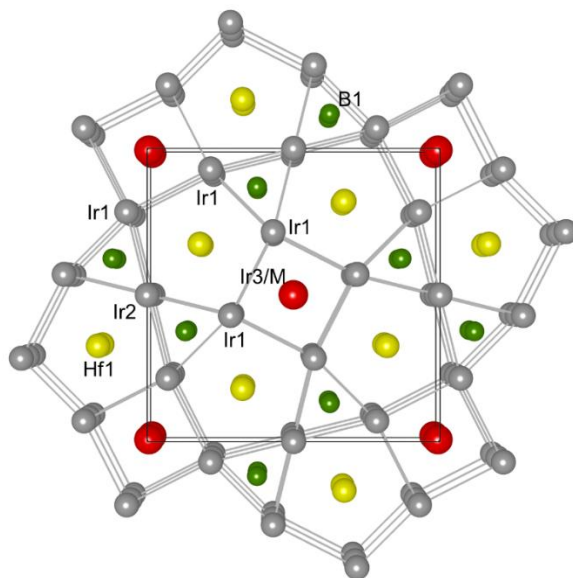


**Figure S1.** Projection along [001] of the crystal structure of  $\text{Hf}_2\text{MIr}_5\text{B}_2$  ( $\text{M} = \text{Fe}, \text{Mn}$ ).

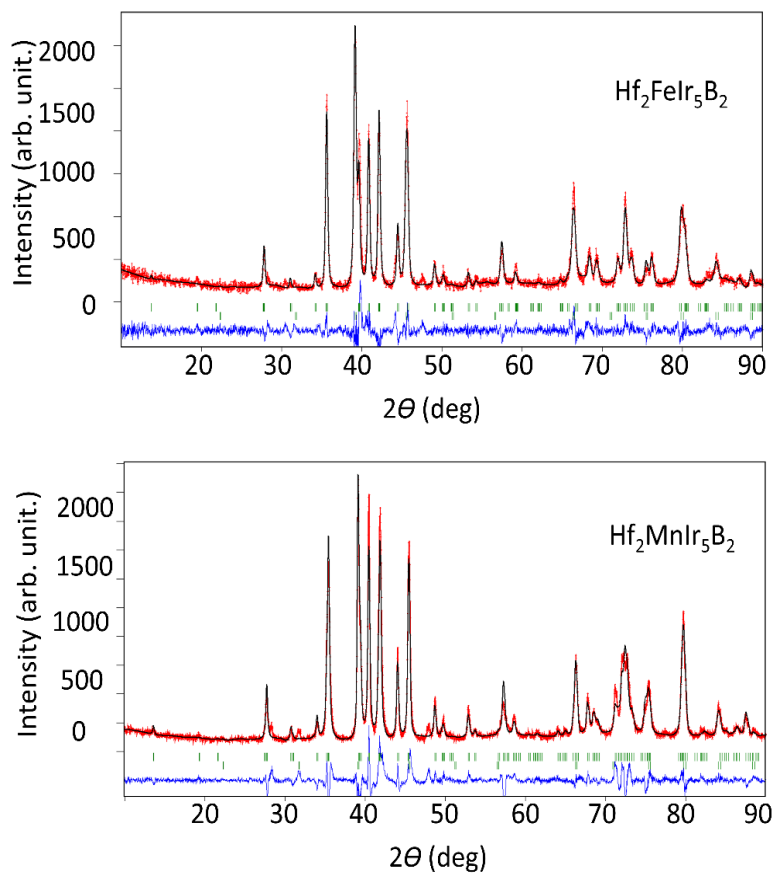


**Figure S2.** *Rietveld* refinement of the powder XRD data. The red and the black curves represent the measured and the calculated patterns, respectively, whereas the blue line shows the intensity difference. The positions of the *Bragg* peaks are shown in green vertical lines (main phase top and side phase  $\text{HfIr}_3\text{B}_{0.5}$  bottom).

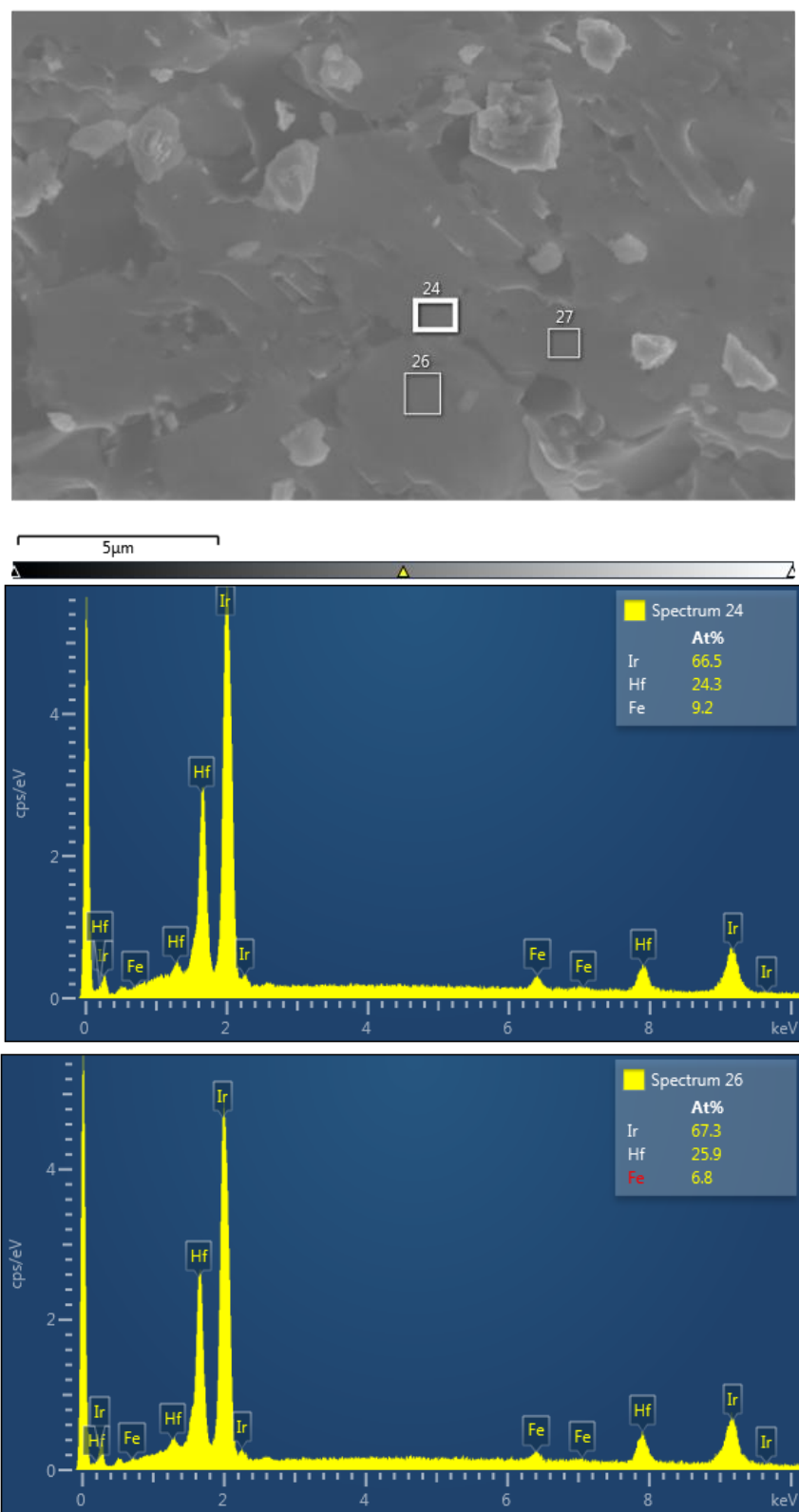


**Figure S3.** SEM image (top) and EDS spectra recorded on as-synthesized crushed samples (after arc-melting) of  $\text{Hf}_2\text{FeIr}_5\text{B}_2$  (spectra 24, 26; average Hf : Fe : Ir = 2 : 0.64 : 5.33).

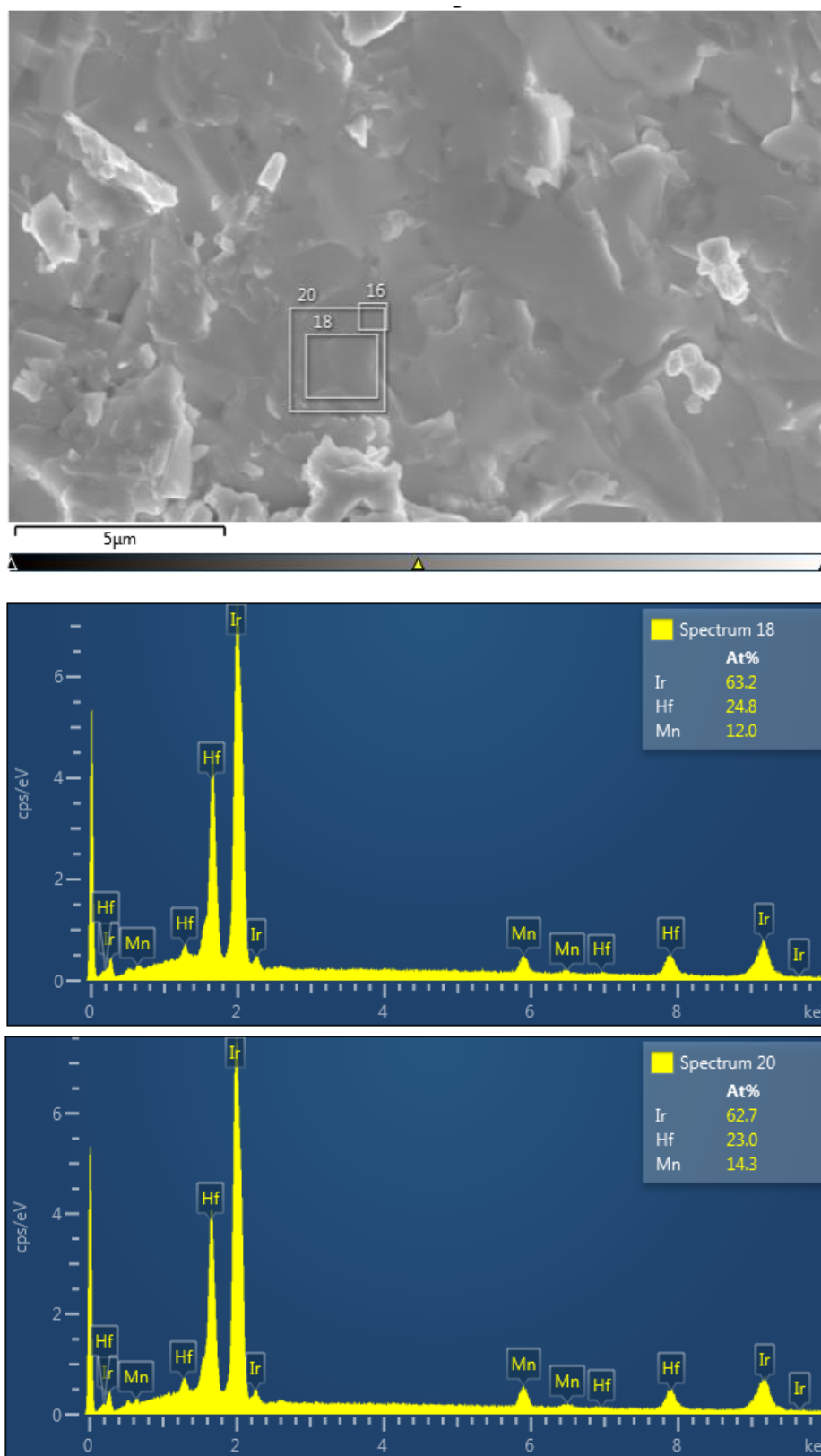


**Figure S4.** SEM image (top left) and EDS spectra recorded on as-synthesized samples (crushed after arc-melting) of  $\text{Hf}_2\text{MnIr}_5\text{B}_2$  (spectra 18, and 20; average Hf : Mn : Ir = 2 : 1.1 : 5.27).

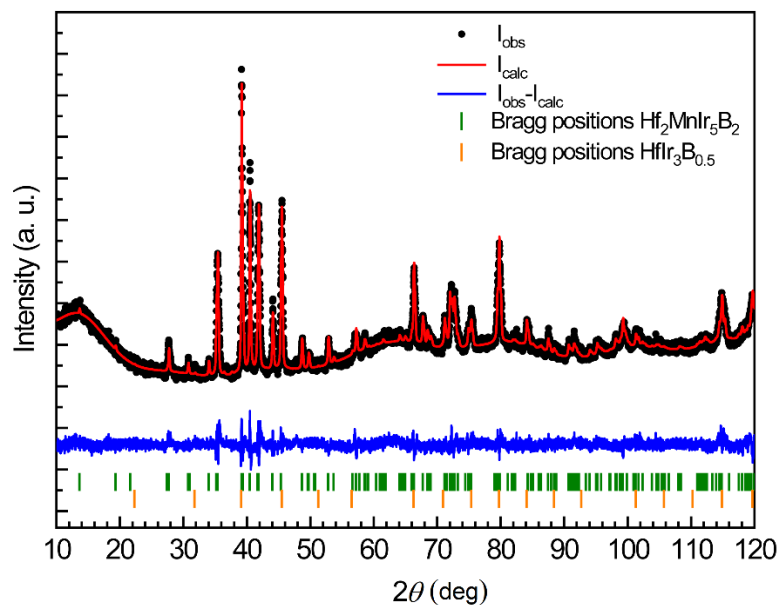


**Figure S5.** *Rietveld* refinement of the powder XRD data of  $\text{Hf}_2\text{MnIr}_5\text{B}_2$  collected on a Bruker D8-A25-Advance diffractometer after magnetic measurements.

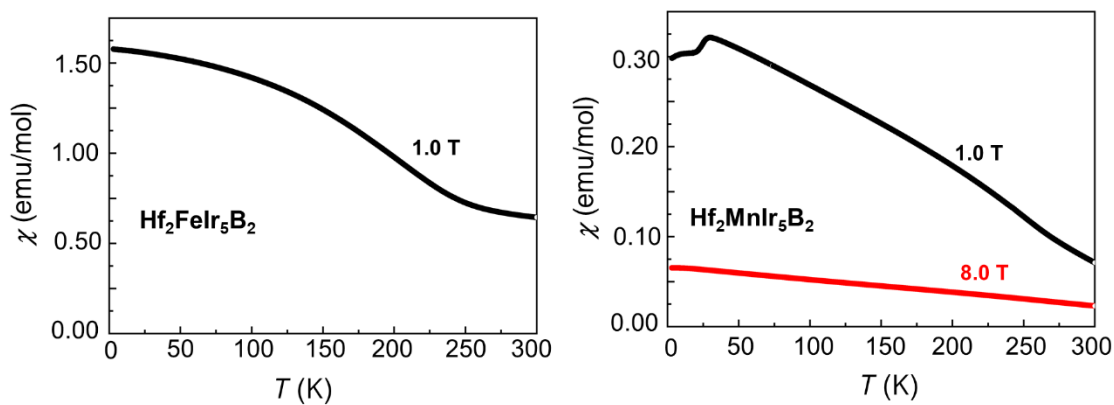


**Figure S6.** Low-temperature magnetic susceptibility plotted as a function of temperature for  $\text{Hf}_2\text{FeIr}_5\text{B}_2$  and  $\text{Hf}_2\text{MnIr}_5\text{B}_2$  measured at 1.0 T and 8.0 T.

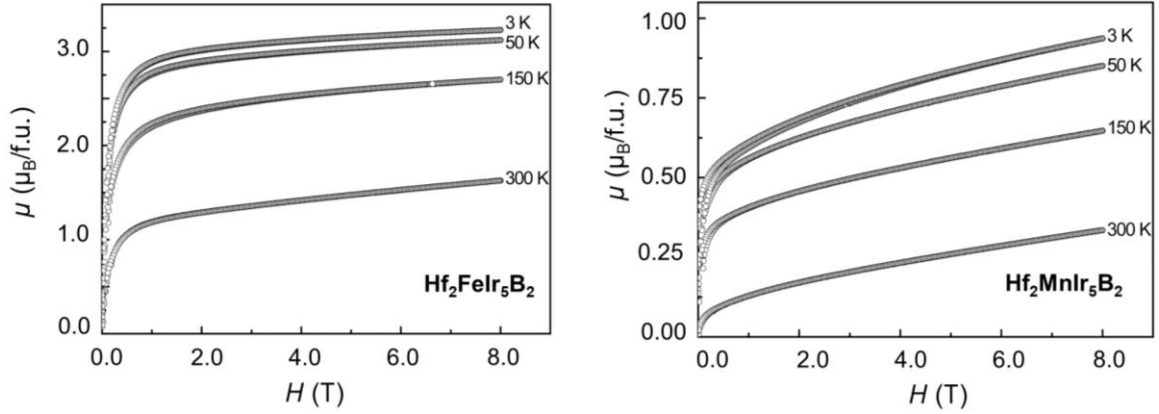


**Figure S7.** Field-dependent magnetization ( $M-H$ ) measurements for  $\text{Hf}_2\text{FeIr}_5\text{B}_2$  and  $\text{Hf}_2\text{MnIr}_5\text{B}_2$  at different temperatures.

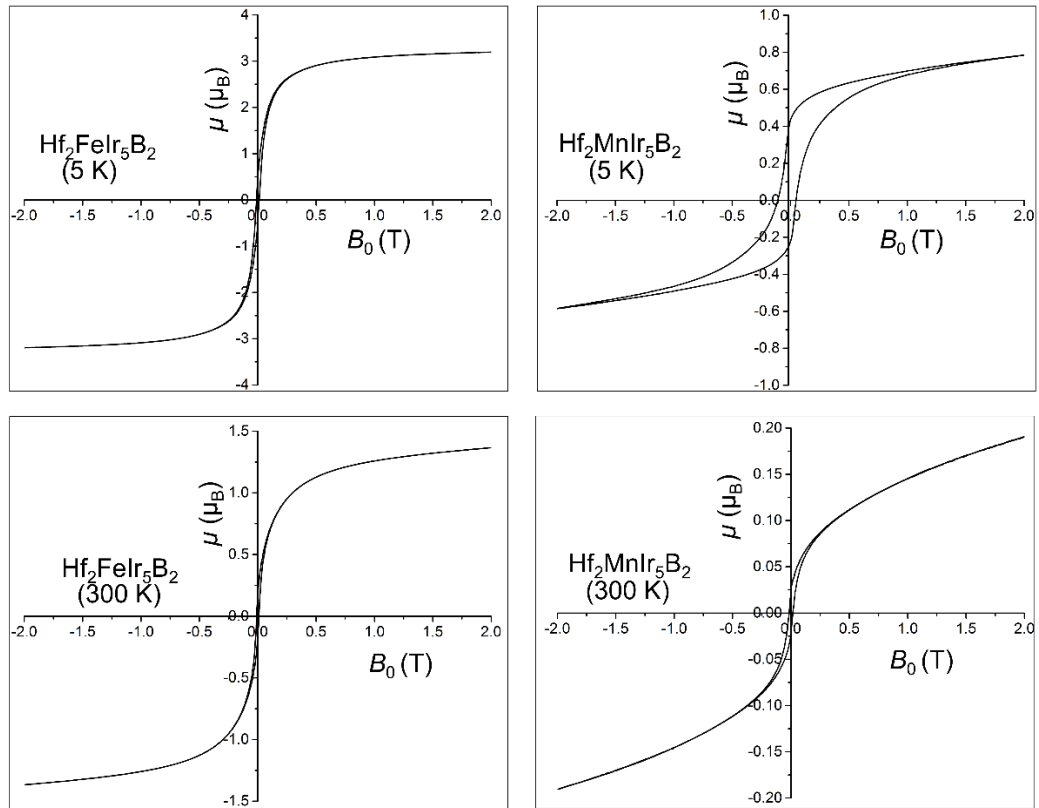


**Figure S8.** Magnetization vs. magnetic field plots (hysteresis loops) measured at 5 and 300 K for  $\text{Hf}_2\text{FeIr}_5\text{B}_2$  and  $\text{Hf}_2\text{MnIr}_5\text{B}_2$ .

## References

- [1] Topas 5, Bruker AXS, Karlsruhe, Germany **2014**.